Proteome-Wide Zika Virus CD4 T Cell Epitope and HLA Restriction Determination

Victoria L. Campbell, LeAnn Nguyen, Elise Snoey, Christopher L. McClurkan, Kerry J. Laing, Lichun Dong, Alessandro Sette, Cecilia S. Lindestam Arlehamn, Danny M. Altmann, Rosemary J. Boyton, Justin A. Roby, Michael Gale Jr, Mars Stone, Michael P. Busch, Phillip J. Norris and David M. Koelle

ImmunoHorizons 2020, 4 (8) 444-453
doi: https://doi.org/10.4049/immunohorizons.2000068
http://www.immunohorizons.org/content/4/8/444

ImmunoHorizons is an open access journal published by
The American Association of Immunologists, Inc.,
1451 Rockville Pike, Suite 650, Rockville, MD 20852

ISSN 2573-7732.

ImmunoHorizons

RESEARCH ARTICLE

Infectious Disease

Proteome-Wide Zika Virus CD4 T Cell Epitope and HLA Restriction Determination

Victoria L. Campbell,[*,1] LeAnn Nguyen,[*,1] Elise Snoey,[*] Christopher L. McClurkan,[*] Kerry J. Laing,[*] Lichun Dong,[*] Alessandro Sette,[†,‡] Cecilia S. Lindestam Arlehamn,[†] Danny M. Altmann,[§] Rosemary J. Boyton,[¶] Justin A. Roby,[‖] Michael Gale, Jr.,[‖,#,] Mars Stone,[††,‡‡] Michael P. Busch,[††,‡‡] Phillip J. Norris,[††,‡‡] and David M. Koelle[*,#,§§,¶¶,‖‖]**

[*]Department of Medicine, University of Washington, Seattle, WA 98195; [†]Division of Vaccine Discovery, La Jolla Institute for Immunology, La Jolla, CA 92037; [‡]Department of Medicine, University of California-San Diego, La Jolla, CA 92093; [§]Department of Immunology and Inflammation, Faculty of Medicine, Imperial College London, London SW7 2AZ, United Kingdom; [¶]Department of Infectious Diseases, Faculty of Medicine, Imperial College London, London SW7 2AZ, United Kingdom; [‖]Center for Innate Immunity of Immune Disease, Department of Immunology, University of Washington, Seattle, WA 98109; [#]Department of Global Health, University of Washington, Seattle, WA 98195; **Department of Microbiology, University of Washington, Seattle, WA 98195; [††]Vitalant Research Institute, San Francisco, CA 94118; [‡‡]Department of Laboratory Medicine, University of California, San Francisco, San Francisco, CA 94143; [§§]Benaroya Research Institute, Seattle, WA 98101; [¶¶]Department of Laboratory Medicine, University of Washington, Seattle, WA 98195; and [‖‖]Vaccine and Infectious Diseases Division, Fred Hutchinson Cancer Research Center, Seattle, WA 98109

ABSTRACT

Zika virus (ZIKV) is a mosquito-borne pathogen that caused an epidemic in 2015–2016. ZIKV-specific T cell responses are functional in animal infection models, and helper CD4 T cells promote avid Abs in the vaccine context. The small volumes of blood available from field research limit the determination of T cell epitopes for complex microbes such as ZIKV. The goal of this project was efficient determination of human ZIKV CD4 T cell epitopes at the whole proteome scale, including validation of reactivity to whole pathogen, using small blood samples from convalescent time points when T cell response magnitude may have waned. Polyclonal enrichment of candidate ZIKV-specific CD4 T cells used cell-associated virus, documenting that T cells in downstream peptide analyses also recognize whole virus after Ag processing. Sequential query of bulk ZIKV-reactive CD4 T cells with pooled/single ZIKV peptides and molecularly defined APC allowed precision epitope and HLA restriction assignments across the ZIKV proteome and enabled discovery of numerous novel ZIKV CD4 T cell epitopes. The research workflow is useful for the study of emerging infectious diseases with a very limited human blood sample availability. *ImmunoHorizons*, 2020, 4: 444–453.

Received for publication July 10, 2020. Accepted for publication July 13, 2020.

Address correspondence and reprint requests to: Dr. David M. Koelle, University of Washington, 750 Republican Street, Room E651, Seattle, WA 98109. E-mail address: dkoelle@medicine.washington.edu

ORCIDs: 0000-0001-6490-5974 (V.L.C.); 0000-0002-9640-8902 (L.N.); 0000-0001-9962-3336 (E.S.); 0000-0001-9245-5325 (K.J.L.); 0000-0001-7302-8002 (C.S.L.A.); 0000-0003-2434-4273 (J.A.R.); 0000-0002-6332-7436 (M.G.); 0000-0001-5619-2767 (M.S.); 0000-0002-1446-125X (M.P.B.); 0000-0003-0526-2088 (P.J.N.); 0000-0003-1255-9023 (D.M.K.).

[1]V.L.C. and L.N. contributed equally to this report.

The sequences presented in this article have been submitted to the Immune Epitope Database and Analysis Resource under accession number 1000842.

This work was supported by National Institutes of Health (NIH) Contracts HHSN272201400049, HHSN268201100001I, HHSN272200900042C, HHSN272201400045C, and 75N93019C00065, and by NIH Grants U01AI151698, R01AI145296, R01AI143265, and R01AI104002.

Abbreviations used in this article: aAPC, artificial APC; AIM, activation-induced marker; ancC, anchored capsid protein; EBV-LCL, EBV-transformed lymphocyte continuous line; ENV, envelope; IEDB, Immune Epitope Database and Analysis Resource; preM, glycosylated precursor of M; TCM, T cell medium.

The online version of this article contains supplemental material.

https://doi.org/10.4049/immunohorizons.2000068

ImmunoHorizons is published by The American Association of Immunologists, Inc.

INTRODUCTION

Acquired, specific T cell immunity is typically required to clear self-limited infections, to maintain an equilibrium with chronic infections, and to enhance functional Ab responses in the vaccination context. Inclusion of microbial Ags that strongly stimulate T cell immunity, and, in particular, specific CD4 T cells are required to trigger lymph node germinal center reactions in which Ag-specific B cells undergo Ig class switching and affinity maturation. T cells typically recognize discrete microbial peptides, termed epitopes. Epitopes are also essential for analytic methods that use peptide–HLA oligomeric reagents, such as tetramers, to analyze pathogen-specific T cells ex vivo. Finally, knowledge of T cell epitopes facilitates therapy using virus-specific T cells that are isolated for adoptive immunotherapy or for the sequencing of their TCRs, which can then be used for transgenic TCR therapy.

Identification of viral T cell epitopes typically uses PBMCs as a source of T cells. Blood contains only a small minority of the total T cells in a human (1) such that T cells that function as T follicular helper cells in lymph node germinal center reactions (2) and tissue-resident memory cells that control infections in barrier tissues (3) might be considered ideal for epitope discovery. These sites are difficult to access, especially in field research conditions during emerging epidemics. It is now recognized, using TCR hypervariable CDR3 sequencing as barcodes for T cell clonotypes, that blood can serve as a surrogate for actual sampling of the T cell repertoire at tissue sites. In the case of Zika virus (ZIKV), infected cells circulate in blood (4) such that T cells may also exert a direct antiviral function in the circulation.

Commonly, T cell epitope discovery methods test peptides from the microbial proteome and use PBMCs for readout. One challenge is that as pathogen genomes increase in size, more and more blood is needed. If T cells recognize diverse epitopes and the integrated size of the response is low, reactivity to individual peptides may fall below the lower limit of detection of direct ex vivo assays. For example, we found that for the large-genome virus HSV-1, only a subset of proven CD4 and CD8 T cell epitopes recognized by blood T cells could be detected by ex vivo IFN-γ ELISPOT (5, 6). Peptide pools can partially mitigate low blood availability, but solubility and solvent toxicity can still be limiting. Follow-up assays and thus more blood are required to definitively show reactivity to single peptides within reactive pools. In addition, techniques, such as intracellular cytokine staining, ELISPOT, and mRNA detection, are cell destructive. Thus, important follow-up work after initial epitope discovery, such as determination of minimal epitopes via truncations, testing for cross-reactivity with peptides from phylogenetically related organisms or strain variants, measurement of functional avidity from peptide dose-response assays, definition of TCR sequences of reactive T cells, and determination of HLA restriction, requires additional blood.

To overcome these obstacles, several groups use T cell surface activation-induced markers (AIM) or surrogates, such as fluorescent dye dilution, for activation to sort live peptide-reactive T cells. After expansion, enriched, live peptide-reactive cells can be used for downstream studies (7). AIM enrichment using peptide stimulation of PBMC does not, however, document T cell reactivity with whole pathogen. Because T cell cross-reactivity to diverse sequence-related and even disparate microbial peptides is ubiquitous (8, 9), it is important to include tests of recognition of the microbial pathogen in the process of T cell epitope determination.

The recent ZIKV epidemic presents an urgent need for vaccine development. Several lines of evidence from animal models suggest that T cells are a functionally important component of the host response to both vaccination and infection (10). We sought to query the ~10,800-nt ZIKV RNA genome encoding a predicted 3423 aa polyprotein using one aliquot of ~10–15 × 10^6 PBMC from ~10 ml of blood. The AIM workflow builds in recognition of whole ZIKV Ag and provides ample T cells for downstream analyses. Using these methods, we have discovered many novel ZIKV CD4 T cell epitopes. The results indicate that broad CD4 recognition of ZIKV in the context of not just HLA-DR but also, frequently, of HLA-DQ and -DP alleles, is consistent with Ag presentation by professional APC in vivo. The response is diverse and includes several proteins in addition to the envelope (ENV) protein important for neutralizing Ab (11). The methods are relevant to field studies for novel and emerging pathogens that are conducted under conditions in which large blood specimens are impractical.

MATERIALS AND METHODS

Cells and viruses

Vero cells (CCL-81) were obtained from American Type Culture Collection (Manassas, VA). The Fortaleza strain of ZIKV was originally provided by Dr. M. Diamond (Washington University, St. Louis, MO). ZIKV was expanded on Vero cells to titers of 1 × 10^7 PFU/ml. PBMC were obtained in Puerto Rico or Florida with consent from adult blood donors identified by screening with serologic/PCR tests for ZIKV infection. Venous blood was processed to PBMC using standard Ficoll centrifugation, and cells were maintained in liquid nitrogen until use. Artificial APC (aAPC) were cell lines transduced to express single human HLA class II heterodimers (Supplemental Table I). aAPC based on RM3 human lymphoma cells (12) were maintained in RPMI 1640 with 10% FCS, 25 mM HEPES, 1% penicillin–streptomycin, 1% nonessential amino acids, and 1 mM sodium pyruvate. Selection for transductants was maintained with 700 μg/ml G418 and 12 μg/ml blasticidin (all from Thermo Fisher Scientific, Waltham, MA). For selected aAPC, HLA expression was induced with 10 μg/ml sodium butyrate (Thermo Fisher Scientific) for 24–48 h prior to testing. aAPC and nontransfected controls based on murine adherent DAP.3 cells were cultured in the same media with 200 μg/ml G418 for transductants. HLA surface expression on transduced cell lines was checked after trypsinizing cells if necessary and staining first with unconjugated anti-pan-HLA-DR, -DP, or -DQ mAbs (13) or no first-Ab negative control, followed by washing and staining with PE-conjugated secondary goat anti-mouse IgG (BioLegend, San Diego, CA) and analyzed by flow cytometry. Some

https://doi.org/10.4049/immunohorizons.2000068

cell lines were checked with PE-Cy7–conjugated anti–HLA-DR clone L243 or relevant isotype control (BioLegend). Only aAPC with HLA expression were used (Supplemental Table II). Cell lines were tested for *Mycoplasma* (MycoAlert; Lonza, Walkersville, MD). Positive cell lines were treated for *Mycoplasma* positivity with ciprofloxacin (10 μg/ml; Hospira, Lake Forest, IL) for 3–4 wk and retested to ensure clearance. EBV-transformed lymphocyte continuous lines (EBV-LCL) were cultured (14) from ~2.5×10^5 donor-thawed PBMC for use as autologous APC.

ZIKV Ags

Vero cells were infected at a multiplicity of infection of ~5. At 48 h, a moderate cytopathic effect was visible. ZIKV- or mock-infected Vero cells were scraped from plastic 75-cm^2 culture flasks and collected by centrifugation at 400 × *g* for 10 min. Supernatant was collected, aliquoted into 100-μl droplets, and UV-C irradiated for 30 min at 10 cm from a GT15T8 bulb for 30 min. Peptides (Supplemental Table II) covered the ZIKV strain Fortaleza proteome (GenBank KX811222.1). These were synthesized as 20-aa-long, overlapping by 10 aa for ZIKV proteins nonstructural protein 1 (NS1), NS3, NS5, and ENV as reported previously (15, 16) (GL Biochem, Shanghai, China). Similar peptides were obtained for the following ZIKV proteins: anchored capsid protein (ancC, also termed C for capsid), glycosylated precursor of M (preM), NS2A, NS2B, NS4A, NS4B, and 2K (GenScript Biotech, Piscataway, NJ). Peptides were dissolved in DMSO (Thermo Fisher Scientific) at 20 mg/ml. Pool stocks of ≤20 peptides containing 1 mg/ml each peptide (detailed in Supplemental Table II) were tested at final concentrations of 1 μg/ml each. Single peptides were tested at specified concentrations.

ZIKV-reactive T cell lines

We modified AIM-based sorting (6, 8, 17–19) to enrich ZIKV-reactive cells. Thawed PBMC were cultured at 2–4 × 10^6 cells per well in 24-well plates in 2 ml/well T cell medium (TCM; RPMI 1640 with 25 mM HEPES, 1% penicillin–streptomycin, 2 mM L-glutamine, 5% FCS [Thermo Fisher Scientific], and 5% human serum [Valley Biomedical, Winchester, VA]). Mock or ZIKV Ags were added at 1:60 dilution for 18 h in humidified, 37°C, 5% CO_2 conditions. Cells were stained with a mixture of anti–CD3-ECD (clone UCHT1; Beckman Coulter, Brea, CA), anti–CD4-PE (clone A161A1; BioLegend), anti–CD8-FITC (clone MHCD0801-4; Thermo Fisher Scientific), anti–CD137-allophycocyanin (clone 4B4-1; BD Biosciences, San Jose, CA), and 7-AAD viability stain (BD Biosciences). Live $CD3^+CD8^-CD4^+CD137^{high}$ cells were sorted (FACSAria II; BD Biosciences). The threshold for CD137 positivity was set using PBMC from separate persons seropositive for HSV-1 and stimulation with UV-treated HSV-1 Ag, as described previously (6). $CD137^{high}$ cells were expanded polyclonally once with PHA as mitogen and further expanded with anti-CD3 mAb as mitogen (19).

T cell functional assays

Bulk responders were tested in [^{3}H]thymidine proliferation assays. For a peptide pool or single peptide to be considered reactive, the response measured as cpm were required to be at least twice that of DMSO negative control, and single peptides were required to be reactive in at least three separate assays at a concentration of 1 μg/ml or lower (below). Triplicate 96-well wells contained 5 × 10^4 autologous EBV-LCL, 5–10 × 10^4 responder cells, and Ag in 200 μl of TCM. On day 3, 0.5 μCi/well [^{3}H]thymidine (PerkinElmer, Waltham, MA) was added, and 18 h later, cells were harvested and counted (TopCount; PerkinElmer). After identification of active 20-aa peptides, triplicate HLA-restricting locus/dose-response assays used 0.01, 0.1, and 1 μg/ml peptide in the absence or presence of blocking anti–HLA-DR, -DP, or -DQ murine mAb or media control. The in-house cell culture supernatant-based mAb preparations were used at a final concentration of 25% (13). HLA-restricting alleles were then studied in triplicate using aAPC (above) and a secreted IFN-γ ELISA readout. For RM3-based aAPC, 5 × 10^4 cells per well were used in 96-well U-bottom plates with responders and peptide, as above. For DAP.3-based aAPC, 3 × 10^4 cells were seeded the day before use into 96-well flat bottom plates, and responders and peptides were added as above. Selected DAP.3 aAPC were treated with 10 μg/ml sodium butyrate diluted from a 1 mg/ml stock in sterile PBS after seeding with a PBS wash prior to adding 1 × 10^5 responder cells. aAPC-based assays used TCM with selective antibiotic discontinuation after T cell addition. After 24 h, supernatants were removed, and IFN-γ was measured (20).

HLA typing

Dried blood spots were provided to Cisco Systems (Seattle, WA), where DNA was extracted, and HLA type was determined by sequencing (21).

Database submission

Epitope-level information, epitope, and assay identification codes are deposited at the Immune Epitope Database and Analysis Resource (IEDB) (22) as submission 1000842.

RESULTS

ZIKV-infected donors

Subjects with PCR-proven ZIKV infection diagnosed in Puerto Rico or Florida in the fall of 2016 were enrolled in the Recipient Epidemiology and Donor Evaluation Study. Characteristics of the Recipient Epidemiology and Donor Evaluation Study design, specimen collection during and after the ZIKV outbreak, and ZIKV PCR and Ab assays have been published (23, 24). Each subject was seropositive for dengue IgG Abs at their initial visit. Six subjects ranging in age from 21 to 70 y old (four women, two men) at the time of ZIKV diagnosis were studied between 82 and 100 d after initial diagnosis (Table I). At this time, all subjects were ZIKV IgG seropositive. Each had been IgM positive at one or more time points, but three had reverted to negative and two were equivocal.

Enrichment of ZIKV-reactive $CD4^+$ T cells

Exposure of PBMC from most ZIKV-immune individuals to cell-associated ZIKV Ag led to a small but detectable increment in live

TABLE I. Participants and specimens used in this study

				PBMC Specimen[a]			HLA Class II			
Donor	Specimen ID	Sex	Age[b]	Day	ZIKV IgG	ZIKV IgM	DRB1	DRB3/4/5	DQB1	DPB1
4	ZVPR8726	F	21	100	pos	pos	*04:11 *13:03	3*01:01 4*01:03	*03:01 *04:02	*04:01 *14:01
10	ZVPR2339	M	54	100	pos	equiv	*11:04 *16:01	3*02:02 5*01:01	*03:01 *05:02	*01:01 *02:01
12	ZVPR6617	F	36	90	pos	equiv	*13:03 *16:01	3*01:01 5*02:02	*03:01 *05:02	*01:01 *10:01
17	ZVPR6947	F	56	88	pos	neg	*04:07 *13:01	3*02:02 4*01:03	*03:02 *06:02	*04:02 *01:05
24	ZVFL4418	F	70	95	pos	neg	*01:01 *15:03	5*01:01	*05:01 *06:02	*01:01 *30:01
28	ZVPR5399	M	52	82	pos	neg	*01:02 *04:11	4*01:03	*03:02 *05:01	*04:02 *01:24

[a]Day of PBMC specimen after initial diagnosis of ZIKV infection and seroreactivity to ZIKV Ag on day of PBMC collection.
[b]Age at time of ZIKV diagnosis.
Abbreviations used in this table: equiv, equivocal; F, female; M, male; neg, negative; pos, positive.

$CD3^+CD4^+CD137^{high}$ lymphocytes at 18 h (representative donor, Fig. 1; summarized in Table II). For some donors, the proportion of CD4 T cells expressing CD137 was <0.01%, and there was no mathematical difference from mock stimulation, but cells were collected regardless. Previously, we used PHA as a functional viability control, leading to CD137 expression by 5–50% of T cells (8, 19). We omitted this to use as many cells as possible for ZIKV stimulation. A small number of activated T cells, ranging from 83 to 354 cells per donor, were sorted (Table II). $CD137^{high}$ cells were expanded polyclonally to $>1 \times 10^8$ cells per donor and frozen as multiple identical aliquots.

Detection of ZIKV epitope-specific CD4 T cells

We detected ZIKV peptide-reactive lymphocytes in five of six T cell lines of $CD137^{high}$ origin. Representative results for subject 24 (Table I) show several positive peptide pools, confirmed in follow-up assays of single peptides (example, Fig. 2). In this case, two adjacent peptides, NS4B aa 13–32 LSHLMGRREGATIGFSMDI and NS4B aa 22–41 EGATIGFSMDIDLRPASAWA (the overlapping region aa 22–32 is underlined and peptides are detailed in Supplemental Table II) were strongly positive, suggesting the presence of T cells recognizing aa 22–32. Reactivity was also noted for the C-terminal adjacent peptide NS4B aa 31–50, indicating that this particular donor recognized at least two discrete epitopes in the N-terminal region of NS4B. In addition, the polyclonal ZIKV-reactive CD4 T cell line also reacted to NS4A aa 73–92 within this pool.

Epitope confirmation and HLA restriction

HLA studies typically began at the locus level, with inclusion of blocking murine mAb capable of inhibiting Ag presentation by all HLA-DR, -DP, or -DQ allelic variants. To improve discrimination, peptides were titrated from 1.0 to 0.01 μg/ml. As representative examples, for subject 24, reactivity to NS4B aa 13–32 and aa 22–41 was nearly completely inhibited by anti–HLA-DQ at each peptide concentration. There was slight inhibition for anti–HLA-DR and no inhibition for anti–HLA-DP (Fig. 3). To determine the HLA-restricting allele, we tested a panel of aAPC expressing subject-specific HLA-DQ as well as -DR molecules. Only aAPC expressing HLA-DQB1*06:02 were able to trigger T cell reactivity, again with identical findings for both overlapping NS4B peptides (Fig. 4). Concordant with the identification of this candidate, the HLA-restricting allele, both longer NS4B peptides, and the shared aa 22–32 region were predicted to tightly bind HLA-DQB1*06:02 using computational algorithms (22).

Integrated CD4 T cell reactivity to ZIKV

The conservative criteria outlined above were used to assign ZIKV epitopes for five participants (Table III). For peptide–participant pairings with peptides that were reactive at least twice at 1 μg/ml but for which HLA restriction could not be determined, epitopes are still considered confirmed. In some cases, no substantial inhibition was noted in anti-HLA blocking mAb experiments. In other cases, restricting HLA loci could be discerned using mAb, but specific alleles could not be demonstrated, given lack of suitable aAPC.

A total of 27 distinct peptides were reactive, including six pairs of adjacent overlapping peptides and one triad of adjacent, overlapping peptides. Peptides NS1 aa 91–110, ancC aa 10–29, and ENV aa 131–150 were found to be antigenic in two donors each. The latter two peptides drove distinct CD4 T cell responses, as the use of aAPC defined restriction by both DPB1*04:01 and DRB1*13:

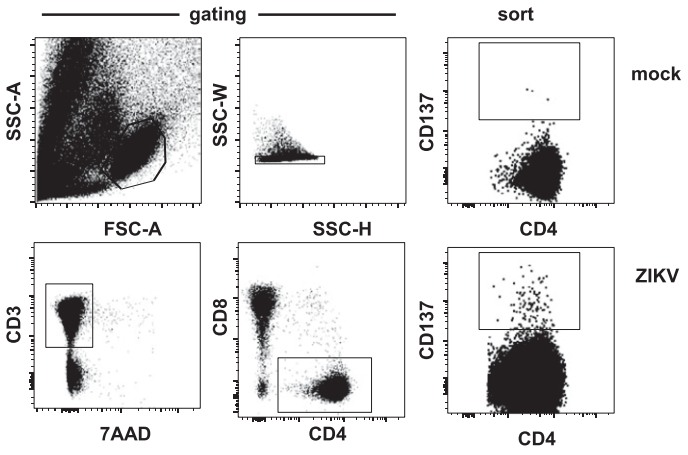

FIGURE 1. Gating scheme of AIM enrichment of polyclonal ZIKV-reactive CD4 T cell lines.

Left four panels illustrate sequential gating scheme of single cells followed by live CD3 T cells and then $CD4^+CD8^-$ cells. At right, in the upper panel, a representative donor shows low CD137 expression 18 h after stimulation with negative control Vero cell preparation and, in contrast, the lower panel shows specific activation of rare CD4 T cells after stimulation with cell-associated, UV-treated ZIKV cell lysate.

TABLE II. ZIKV activation-induced, marker-sorted CD4 T cells

Donor	Specimen Identification	Mock[a]	ZIKV[a]	CD137^{high} Cells[b]
4	ZVPR8726	<0.01	<0.01	83
10	ZVPR2339	0	0.1	122
12	ZVPR6617	<0.01	<0.01	175
17	ZVPR6947	0.01	0.02	161
24	ZVFL4418	0.04	0.06	301
28	ZVPR5399	0.08	0.10	354

[a]Percentage of live, lymphocyte-gated, $CD3^+CD4^+CD8^-$ cells expressing CD137 in response to mock or ZIKV Ag.
[b]Cell-sorter count of live $CD3^+CD4^+CD8^-CD137^{high}$ cells sorted in cells with ZIKV Ag.

01 for ancC aa 10–29 and by both DPB1*02:01 and DRB1*01:01 for ENV aa 131-150. Taken together, these data imply CD4 T cell responses to between 23 and 29 ZIKV epitopes. The presence of more than one HLA-restricting locus and allele for some individual subject/peptides combinations (Table III) likely indicates a polyclonal response. For example, for subject 17, polyclonal CD4 T cells reacted to peptide NS1 81–100 ENGVQLTVVVGSVKNPMWRG in the context of autologous EBV-LCL used as an APC. aAPC analyses showed that both DRA1*01:01/DRB1*13:01 and DQA1*01:02/DQB1*06:02 heterodimers were able to present this 20-aa peptide to the expanded $CD137^{high}$ CD4 T cell population (Fig. 4). Dual recognition of some 20-aa-long peptides, presumably by distinct T cell clonotypes, was supported by the presence of peptides with high predicted binding avidity for each implicated peptide. Using the NetMHCPan3.2 predictive algorithm (25), hosted at IEDB, for this example, NS1 81–100 contained internal peptides predicted to tightly bind to a peptide internal to both implicated HLA-restricting alleles (Fig. 4). Without conducting truncation analyses within overlapping antigenic peptides combined with query with aAPC, including creation of CD4 T cell clones, the complexity of responses contained with these polyclonal T cell lines can only be estimated.

Given these levels of complexity, epitope counts and descriptions of Ag immunodominance and epitope diversity remain somewhat ambiguous. The number of reactive peptides detected ranged from two (donor 12) to 12 (donor 17) per participant (Table III). Overall, reactivity was present in each structural protein derived by proteolysis of the ZIKV polyprotein (ancC, preM, and ENV) and in five nonstructural proteins (NS1, NS2B, NS4A, NS4B, and NS5). Among these, ENV and NS1 were the most frequently recognized. Although the specific HLA-restricting alleles reflected the subjects studied, there was fairly even representation of HLA-DR, -DP, and -DQ loci, which restricted responses to 9, 8, and 10 peptides, respectively.

DISCUSSION

ZIKV caused globally widespread infections in regions hospitable to insect vectors in 2015–2016. During this crisis, children of thousands of pregnant women suffered profound neurodevelopmental damage related to ZIKV crossing the placenta and infecting embryonic brain cells (26). This has led to great interest in vaccine development, with a principle goal of high-titer neutralizing Ab (11). Recognizing the essential role of helper CD4 T cells in the development of long-lasting and highly avid Abs, it is generally agreed that vaccines should at a minimum elicit substantial CD4 T cell responses. In addition, T cells can have important antiviral effector functions in animal models of ZIKV and other flavivirus infections (27). Therefore, there has been intensive research into the antigenic targets, phenotype, and *Flaviviridae* cross-reactivity

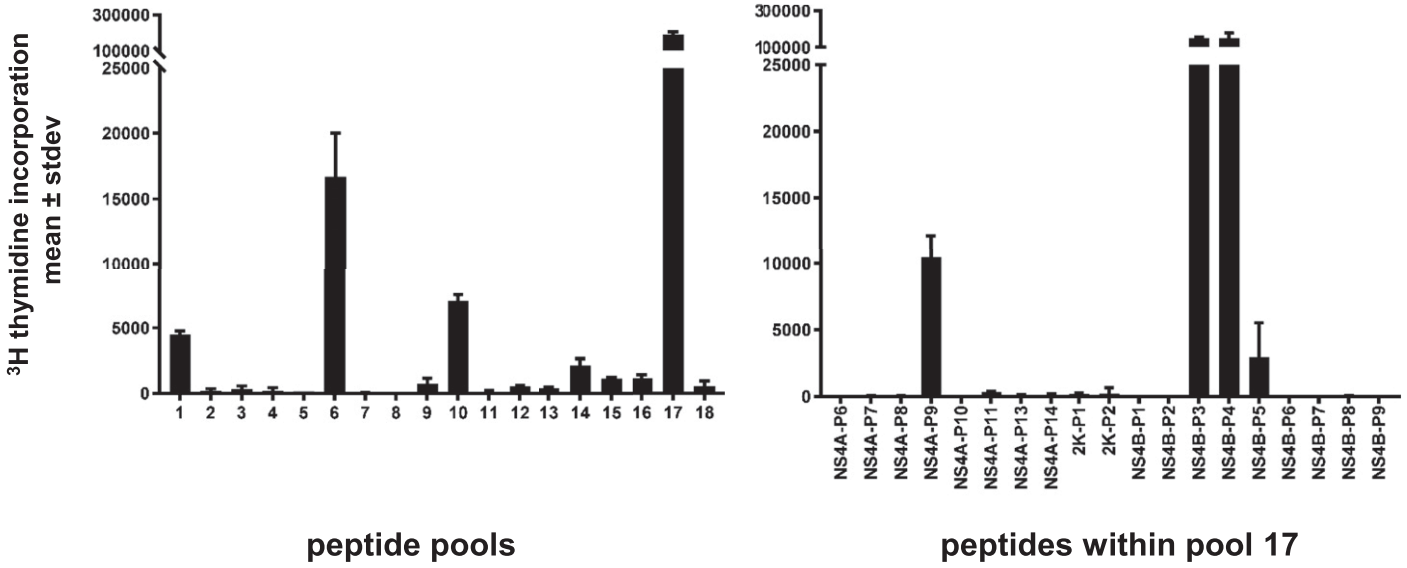

FIGURE 2. Definition of ZIKV peptides recognized by polyclonal ZIKV-reactive CD4 T cell lines enriched from ZIKV-seropositive donors.
At left, the AIM-enriched bulk T cells from donor 24 were queried with pooled proteome-covering ZIKV peptides using autologous EBV-LCL as APC. At right, single peptides within pool 17 were tested. Assays were performed in triplicate and expressed as SD of the mean.

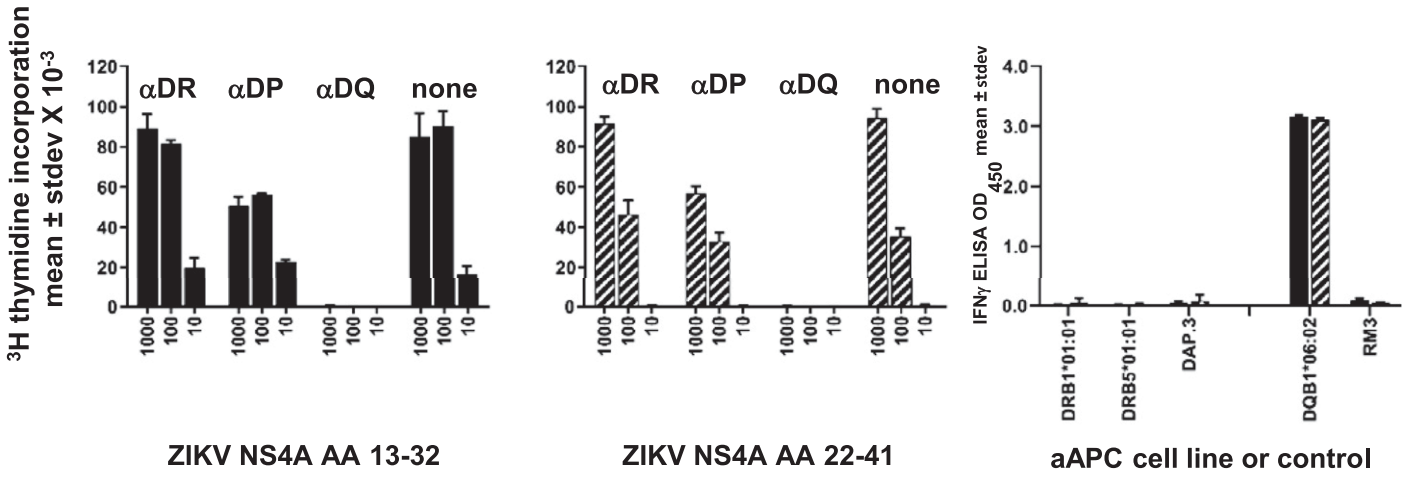

FIGURE 3. Example of determination of HLA-restricting locus and allele.

Left two panels show reactivity of polyclonal ZIKV-reactive CD4 T cells from donor 24 to the indicated peptides in proliferation assays using autologous EBV-LCL as APC. Peptide identities and titrations from 1 to 0.01 μg/ml (1000–10 ng/ml) are indicated on the *x*-axis. Anti-HLA class II mAbs or no Ab control used to test inhibition are indicated at top. Anti–HLA-DQ inhibited the response to both peptides. Right panel shows IFN-γ secretion by the same effector cells in response to 1 μg/ml peptide NS4A aa 13–32 (black bars) and aa 22–41 (hatched bars) using defined aAPC expressing donor-specific HLA alleles. Only RM3 cells expressing DQB1*06:02 were active.

of human ZIKV-specific T cells in both the infection and vaccine contexts (24, 28).

ZIKV is representative of epidemic and pandemic viral infections that periodically cause great morbidity, mortality, and economic damage. Once a pathogen's nucleic acid sequence is identified, rapid determination of immunodominant T cell epitopes is essential for study of the immune correlates of infection severity and possible immunopathology, and as a benchmark for candidate vaccines. Although blood sampling is accepted for medical purposes, health conditions, such as anemia, and cultural standards may limit blood donations for research (29). Even if generous amounts of research blood are available, some important pathogens, such as *Mycobacterium tuberculosis* or *Herpesviridae*, have quite large genomes, such that direct ex vivo study of the entire predicted proteome is impractical and expensive. Strategies to mitigate this include preliminary epitope mapping using large PBMC harvests from consenting, immune donors and creation of large peptide pools ("megapools") from accreted, documented peptide epitopes (30, 31). Related approaches use predictive algorithms to define peptides that can bind a set of population-prevalent HLA-allelic variants and assemble megapools across the pathogen's proteome (32). These pathways, although yielding much data, are limited to the HLA types included in the epitope discovery or prediction pipelines that contribute to pool creation and do not provide confirmation of T cell recognition of the microbe.

In addition to these practical and medical considerations, the magnitude of the pathogen-specific T cell response, especially at memory time points, can be very low, providing an additional challenge to direct ex vivo approaches. For example, the integrated abundance of HHV-6B–reactive CD4 T cells in PBMC is on the order of 0.05% (19). Using cells expressing multiple AIM molecules (CD137, CD69, and CD154), we were able to reliably enrich virus-reactive cells to levels of up to 50% (19). This ZIKV project featured both low immune responses and very limited blood volumes. After addition of ZIKV Ag, both the absolute magnitude and increment above negative control for CD137 expression by CD4 T cells was minuscule or too small to detect (Fig. 1, Table II).

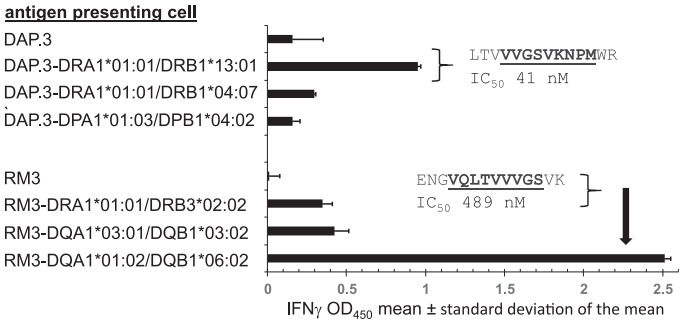

FIGURE 4. CD4 T cell recognition of ZIKV peptide NS1 81–100 is restricted by two distinct HLA alleles.

APC expressing defined HLA class II heterodimers or nonexpressing parental cells DAP.3 or RM3 (at left) were incubated with 20-mer peptide NS 81–100, washed, and cocultured with expanded polyclonal CD4 T cells enriched using CD137 expression after contact with whole UV-treated ZIKV viral lysate. Data from triplicate assays are mean and SD of IFN-γ secretion at 24 h, as measured by ELISA. Insets are 14–15 aa peptides internal to NS1 81–100 and their predicted binding to the indicated HLA heterodimers, with core HLA binding motifs bold and underlined. The vertical arrow in the lower portion connects the peptide sequence with HLA DQA1*01:02/DQB1*06:02, the heterodimer used to predict the IC_{50} value in the figure.

TABLE III. T cell epitopes in ZIKV detected using bulk ZIKV viral lysate-reactive CD4 T cell lines

Donor	Protein (aa)	Sequence	HLA Loci[a]	HLA-Restricting Allele(s)[b]
4	ENV (301–320)	KGVSYSLCTAAFTFTKIPAE	DP	HLA-DPB1*04:01
4	NS1 (91–110)	GSVKNPMWRGPQRLPVPVNE	DP	HLA-DPB1*04:01
4	NS1 (101–120)	PQRLPVPVNELPHGWKAWGK	DP	HLA-DPB1*04:01
4	NS2B (36–55)	GLLIVSYVVSGKSVDMYIER	DR	HLA-DRB1*04:11
10	ancC (10–29)	GFRIVNMLKRGVARVSPFGG		HLA-DPB1*02:01
10	ancC (82–101)	KKFKKDLAAMLRIINARKEK		
10	ENV (101–120)	WGNGCGLFGKGSLVTCAKFA		HLA-DQB1*03:01
10	ENV (111–130)	GSLVTCAKFACSKKMTGKSI		HLA-DRB3*02:02
10	ENV (131–150)	QPENLEYRIMLSVHGSQHSG		HLA-DPB1*02:01
10	NS1 (141–160)	KECPLKHRAWNSFLVEDHGF		
12	NS1 (31–50)	RYKYHPDSPRRLAAAVKQAW	DR	
12	NS1 (91–110)	GSVKNPMWRGPQRLPVPVNE	DP	
17	ancC (10–29)	GFRIVNMLKRGVARVSPFGG	DR	HLA-DRB1*13:01
17	ancC (37–56)	LLLGHGPIRMVLAILAFLRF	DR	
17	ancC (46–65)	MVLAILAFLRFTAIKPSLGL	DR/DP	HLA-DRB1*13:01
17	ENV (61–80)	YEASISDMASDSRCPTQGEA	DQ	HLA-DQB1*03:02
17	ENV (391–410)	VGEKKITHHWHRSGSTIGKA	DR	HLA-DRB1*04:07
17	NS1 (81–100)	ENGVQLTVVVGSVKNPMWRG	DQ	HLA-DRB1*13:01, HLA-DQB1*06:02
17	NS1 (151–170)	NSFLVEDHGFGVFHTSVWLK	DP	HLA-DPB1*04:02, HLA-DQB1*03:02
17	NS1 (161–180)	GVFHTSVWLKVREDYSLECD	DP	HLA-DPB1*04:02, HLA-DQB1*03:02
17	NS1 (201–220)	WIESEKNDTWRLKRAHLIEM		HLA-DPB1*04:02
17	NS5 (221–240)	WVSGAKSNTIKSVSTTSQLL	DR	HLA-DRB1*04:07, HLA-DRB1*13:01
17	PreM (64–83)	DVDCWCNTTSTWVVYGTCHH	DQ	HLA-DQB1*06:02
17	PreM (73–92)	STWVVYGTCHHKKGEARRSR	DQ	HLA-DQB1*06:02
24	ENV (131–150)	QPENLEYRIMLSVHGSQHSG	DR	HLA-DRB1*01:01
24	NS4A (73–92)	MRNKGIGKMGFGMVTLGASA	DQ	HLA-DQB1*06:02
24	NS4B (13–32)	LSHLMGRREEGATIGFSMDI	DQ	HLA-DQB1*06:02
24	NS4B (22–41)	EGATIGFSMDIDLRPASAWA	DQ	HLA-DQB1*06:02
24	NS4B (31–50)	DIDLRPASAWAIYAALTTFI		
24	NS5 (41–60)	RRALKDGVATGGHAVSRGSA	DR	HLA-DRB1*01:01, HLA-DRB5*01:01

[a]Specificity of HLA locus-specific mAb or mAbs causing substantial inhibition of proliferative responses by bulk ZIKV-reactive CD4 T cell lines in [^{3}H]thymidine incorporation assays. In some instances, inhibition was not noted with any anti-HLA mAb, whereas in others, more than one mAb led to inhibition.
[b]HLA loci expressed by aAPC, leading to specific secretion of IFN-γ by bulk ZIKV-reactive CD4 T cell lines. In some instances, reactive aAPC were not detected.

Lack of PBMC to use as APC to query expanded, CD137^{high} polyclonal CD4 T cell lines, a quality control step used for several pathogens (6, 8, 19), necessitated direct progression to ZIKV peptide screens without this reassurance. Peptides covering the predicted proteome were obtained for this purpose. Culture of autologous EBV-LCL from the equivalent of 0.25 ml of blood, although requiring a few weeks, provided an ongoing source of APC for tests of fine specificity, and is a simple procedure. Overall, despite the low levels of memory CD4 T cell responses, we identified up to 30 CD4 T cell epitopes from ~10 ml of blood per donor from five donors. The essentially limitless supply of responder cells and autologous aAPC, HLA typing, and a bank of aAPC expressing defined HLA class II heterodimers further allowed us to assign definitive HLA restriction to the majority of epitopes.

Supernatant-derived ZIKV Ag was able to restimulate rare CD4 T cells from PBMC that recognize not only abundant structural ZIKV Ags, such as ENV and ancC, but also nonstructural proteins not thought to be present in virions. Overall, epitopes detected in nonstructural proteins outnumbered those detected from classic structural proteins. It is possible that small amounts of viral proteins categorized as nonstructural were in fact contained within virions. A survey of the literature reveals very little proteomic study of ZIKV virions. Nonstructural proteins could also be shed into the supernatant. It is also interesting that prominent restriction by HLA-DQ and -DP alleles, in addition to HLA-DR, was documented in our small specimen set. This may correlate with in vivo infection of monocytes, as these cells constitutively express each of these HLA class II gene products (33). Although definition of CD4 T cell epitopes in ZIKV is relatively mature, the precise HLA restriction of many epitopes has not been demonstrated experimentally.

The use of a related, somewhat reversed workflow, starting with polyclonal enrichment and expansion of peptide-reactive cells, followed by readout with ZIKV-infected APC, has been successful for both flavivirus-immune and naive blood donors. Effector CD4 T cell lines from dengue-immune, ZIKV-naive donors specific for cross-reactive peptides showed brisk cytokine and granzyme B responses to HLA-appropriate, allogeneic EBV-LCL APC infected with an African strain of ZIKV (34). We plan to examine the cytotoxic and other effector potential of ZIKV-reactive CD4 T cells in response to ZIKV-infected APC in future studies. In other viral systems, we have been able to readily clone and expand T cell clones from AIM-enriched T cell lines, perhaps because of the strongly costimulatory effect of CD137 ligation with an mAb that is integral to initial AIM cell sorting (17, 35). Clones with fully defined specificity and HLA restriction should enable us to determine whether physiologically relevant cells with

limited HLA class II expression can be recognized by virus-specific CD4 T cells in the context of viral infection. Unfortunately, we were not able to correlate T cell responses with clinical outcomes because of our small sample size and because the cell donors were recruited from a blood donation program. Precisely defined T cell epitopes are a necessary precursor for direct ex vivo studies with peptide–MHC staining reagents, an important method for establishing immune correlates of infection severity (36, 37).

Limited blood samples and logistics required us to cryopreserve PBMC. Some cells with the ability to present complex Ags, such as plasmacytoid dendritic cells, are sensitive to freeze–thaw and are studied fresh (38). However, plasmacytoid dendritic cells are generally thought to have primarily innate immunity functions, whereas other blood leukocytes mediate most Ag presentation to CD4 T cells. AIM work by our laboratory and others to enrich or measure virus-specific CD4 T cell responses to peptide or complex Ags generally uses cryopreserved PBMC (6, 8, 19, 32, 39, 40). This indicates that cells with APC function do survive freeze–thaw, whereas not ruling out a decrement. Limited research comparing cryopreserved with fresh PBMC for CD4 T cell recall to complex Ags is consistent with some decrease in magnitude of responses but retention of proportionality within the results (41, 42). Although the use of cryopreserved PBMC is almost universal in human T cell research requiring complex cohorts, rare donors, and biocontainment, future research could compare responses between fresh and cryopreserved cells.

We were not able to include flavivirus-naive individuals in our study. However, we feel it is unlikely that the epitope-specific responses we detected came from the naive repertoire. In studies of replication-competent flavivirus vaccines, such as yellow fever virus strain 17D and attenuated dengue, that were conducted in flavivirus-naive individuals, virus-reactive T cells were essentially undetectable at baseline (43, 44). We found that HSV- and CMV-seronegative persons had very low or undetectable virus-specific T cells in PBMC, using direct ex vivo tests, including CD137-based AIM (6, 38). Further research will be required to determine whether the one-step restimulation used in this report was able to amplify naive responses, which are reported to be present but in very low abundance in virus-seronegative humans (45).

The parameters chosen for rare cell enrichment were tailored to both the use of complex viral Ag as the initial stimulus and to the biology of CD137 upregulation after stimulation of T cells. Typically, direct ex vivo assays to detect recall responses can use shorter times, on the order of 6–8 hours, for peptides, whereas for complex Ags that require intracellular processing within APC, longer periods are used. Studies show that 18–24 hours or more is optimal for CD137 upregulation regardless of whether peptide of complex Ags are used (7, 43, 46). These data inform the protocols used for CD137-based rare cell enrichment and quantitative assays (32, 39).

Our findings significantly extend previous communications concerning the specificity of ZIKV-reactive T cells. Koblischke et al. (47) used 15-mer overlapping peptides covering the ZIKV C, preM, and ENV proteins and detected IL-2 secretion in ex vivo ELISPOT from CD8-depleted PBMC. The donors were ZIKV-positive travelers returned from ZIKV epidemic regions with prior flavivirus vaccination with live attenuated tick-born encephalitis or yellow fever; all were dengue-seronegative. Compared with flavivirus-naive controls, positive responses to ZIKV peptides segregated with ZIKV-immune status and across the cohort were detected for each ZIKV gene studied (47). Data integration with CD4 T cell epitopes in the IEDB (22) identified several putative immunogenic regions, including ENV 101–150, 301–320 and 391–410, NS1 151–180, and ancC 37–56 and 82–101 that overlap with epitope regions described in this study. Previous studies summarized in the IEDB identified 89 different Zika-derived CD4 epitopes, ~30% (n = 25) of which cluster (48) with the epitopes identified in the current study. However, exact MHC restriction has been defined for just 10 of the previously defined epitopes. By comparison, the present analysis has identified 27 different reactive peptide epitopes, of which 18 are novel, associated with 29 unique HLA class II epitope restrictions, none of which have been previously described. Thus, the current study has contributed a 3-fold increase in the number of defined Zika CD4-epitope HLA class II restrictions that can subsequently be used for generation of multimeric reagents to further characterize Zika CD4 responses.

In conclusion, the level of ZIKV-reactive memory CD4 T cells expressing the activation marker CD137 in response to whole viral recall Ag in healthy, dengue-seropositive adults, several months after ZIKV infection, was quite low. Regardless, CD137 AIM-based virus-specific CD4 T cell enrichment led to readily expandable, polyclonal cell populations that contained epitope-specific, ZIKV-specific CD4 T cell recovery from the majority of donors. Importantly, very small blood samples, acceptable in diverse communities, were able to yield valuable viral T cell epitope information, including precise HLA restriction information.

DISCLOSURES

The authors have no financial conflicts of interest.

REFERENCES

1. Morris, S. E., D. L. Farber, and A. J. Yates. 2019. Tissue-resident memory T cells in mice and humans: towards a quantitative ecology. *J. Immunol.* 203: 2561–2569.
2. Heit, A., F. Schmitz, S. Gerdts, B. Flach, M. S. Moore, J. A. Perkins, H. S. Robins, A. Aderem, P. Spearman, G. D. Tomaras, et al. 2017. Vaccination establishes clonal relatives of germinal center T cells in the blood of humans. *J. Exp. Med.* 214: 2139–2152.
3. Gebhardt, T., P. G. Whitney, A. Zaid, L. K. Mackay, A. G. Brooks, W. R. Heath, F. R. Carbone, and S. N. Mueller. 2011. Different patterns of peripheral migration by memory CD4+ and CD8+ T cells. *Nature* 477: 216–219.
4. Foo, S. S., W. Chen, Y. Chan, J. W. Bowman, L. C. Chang, Y. Choi, J. S. Yoo, J. Ge, G. Cheng, A. Bonnin, et al. 2017. Asian Zika virus strains target CD14^{+} blood monocytes and induce M2-skewed immunosuppression during pregnancy. *Nat. Microbiol.* 2: 1558–1570.
5. Jing, L., J. T. Schiffer, T. M. Chong, J. J. Bruckner, D. H. Davies, P. L. Felgner, J. Haas, A. Wald, G. M. G. M. Verjans, and D. M. Koelle. 2013. CD4 T-cell memory responses to viral infections of humans show

pronounced immunodominance independent of duration or viral persistence. *J. Virol.* 87: 2617–2627.

6. Jing, L., J. Haas, T. M. Chong, J. J. Bruckner, G. C. Dann, L. Dong, J. O. Marshak, C. L. McClurkan, T. N. Yamamoto, S. M. Bailer, et al. 2012. Cross-presentation and genome-wide screening reveal candidate T cells antigens for a herpes simplex virus type 1 vaccine. [Published erratum appears in 2012 *J. Clin. Invest*. 122: 3024.] *J. Clin. Invest*. 122: 654–673.
7. Wolfl, M., J. Kuball, W. Y. Ho, H. Nguyen, T. J. Manley, M. Bleakley, and P. D. Greenberg. 2007. Activation-induced expression of CD137 permits detection, isolation, and expansion of the full repertoire of CD8+ T cells responding to antigen without requiring knowledge of epitope specificities. *Blood* 110: 201–210.
8. Nayak, K., L. Jing, R. M. Russell, D. H. Davies, G. Hermanson, D. M. Molina, X. Liang, D. R. Sherman, W. W. Kwok, J. Yang, et al. 2015. Identification of novel *Mycobacterium tuberculosis* CD4 T-cell antigens via high throughput proteome screening. *Tuberculosis (Edinb.)* 95: 275–287.
9. Clute, S. C., L. B. Watkin, M. Cornberg, Y. N. Naumov, J. L. Sullivan, K. Luzuriaga, R. M. Welsh, and L. K. Selin. 2005. Cross-reactive influenza virus-specific CD8+ T cells contribute to lymphoproliferation in Epstein-Barr virus-associated infectious mononucleosis. *J. Clin. Invest*. 115: 3602–3612.
10. Grubor-Bauk, B., D. K. Wijesundara, M. Masavuli, P. Abbink, R. L. Peterson, N. A. Prow, R. A. Larocca, Z. A. Mekonnen, A. Shrestha, N. S. Eyre, et al. 2019. NS1 DNA vaccination protects against Zika infection through T cell-mediated immunity in immunocompetent mice. *Sci. Adv.* 5: eaax2388.
11. Erasmus, J. H., A. P. Khandhar, J. Guderian, B. Granger, J. Archer, M. Archer, E. Gage, J. Fuerte-Stone, E. Larson, S. Lin, et al. 2018. A nanostructured lipid carrier for delivery of a replicating viral RNA provides single, low-dose protection against Zika. *Mol. Ther.* 26: 2507–2522.
12. McKinney, D. M., S. Southwood, D. Hinz, C. Oseroff, C. S. Arlehamn, V. Schulten, R. Taplitz, D. Broide, W. A. Hanekom, T. J. Scriba, et al. 2013. A strategy to determine HLA class II restriction broadly covering the DR, DP, and DQ allelic variants most commonly expressed in the general population. *Immunogenetics* 65: 357–370.
13. Koelle, D. M., L. Corey, R. L. Burke, R. J. Eisenberg, G. H. Cohen, R. Pichyangkura, and S. J. Triezenberg. 1994. Antigenic specificities of human CD4+ T-cell clones recovered from recurrent genital herpes simplex virus type 2 lesions. *J. Virol.* 68: 2803–2810.
14. Tigges, M. A., D. Koelle, K. Hartog, R. E. Sekulovich, L. Corey, and R. L. Burke. 1992. Human CD8+ herpes simplex virus-specific cytotoxic T-lymphocyte clones recognize diverse virion protein antigens. *J. Virol.* 66: 1622–1634.
15. Reynolds, C. J., O. M. Suleyman, A. M. Ortega-Prieto, J. K. Skelton, P. Bonnesoeur, A. Blohm, V. Carregaro, J. S. Silva, E. A. James, B. Maillère, et al. 2018. T cell immunity to Zika virus targets immunodominant epitopes that show cross-reactivity with other Flaviviruses. *Sci. Rep.* 8: 672.
16. Reynolds, C. J., P. Watber, C. N. O. Santos, D. R. Ribeiro, J. C. Alves, A. B. L. Fonseca, A. J. B. Bispo, R. L. S. Porto, K. Bokea, A. M. R. de Jesus, et al. 2020. Strong CD4 T cell responses to Zika virus antigens in a cohort of dengue virus immune mothers of congenital Zika virus syndrome infants. *Front. Immunol.* 11: 185.
17. Jing, L., K. J. Laing, L. Dong, R. M. Russell, R. S. Barlow, J. G. Haas, M. S. Ramchandani, C. Johnston, S. Buus, A. J. Redwood, et al. 2016. Extensive CD4 and CD8 T cell cross-reactivity between alphaherpesviruses. *J. Immunol.* 196: 2205–2218.
18. Ramchandani, M. S., L. Jing, R. M. Russell, T. Tran, K. J. Laing, A. S. Magaret, S. Selke, A. Cheng, M. L. Huang, H. Xie, et al. 2019. Viral genetics modulate orolabial herpes simplex virus type 1 shedding in humans. *J. Infect. Dis.* 219: 1058–1066.
19. Hanson, D. J., O. Tsvetkova, G. F. Rerolle, A. L. Greninger, A. Sette, L. Jing, V. L. Campbell, and D. M. Koelle. 2019. Genome-wide approach to the CD4 T-cell response to human herpesvirus 6B. *J. Virol.* 93: e00321-19.
20. Koelle, D. M., H. B. Chen, M. A. Gavin, A. Wald, W. W. Kwok, and L. Corey. 2001. CD8 CTL from genital herpes simplex lesions: recognition of viral tegument and immediate early proteins and lysis of infected cutaneous cells. *J. Immunol.* 166: 4049–4058.
21. Lind, A., O. Akel, M. Wallenius, A. Ramelius, M. Maziarz, L. P. Zhao, D. E. Geraghty, L. Palm, Å. Lernmark, and H. E. Larsson. 2019. HLA high-resolution typing by next-generation sequencing in Pandemrix-induced narcolepsy. *PLoS One* 14: e0222882.
22. Vita, R., J. A. Overton, J. A. Greenbaum, J. Ponomarenko, J. D. Clark, J. R. Cantrell, D. K. Wheeler, J. L. Gabbard, D. Hix, A. Sette, and B. Peters. 2015. The Immune Epitope Database (IEDB) 3.0. *Nucleic Acids Res.* 43: D405–D412.
23. Kleinman, S., M. P. Busch, E. L. Murphy, H. Shan, P. Ness, and S. A. Glynn; National Heart, Lung, and Blood Institute Recipient Epidemiology and Donor Evaluation Study (REDS-III). 2014. The national heart, lung, and blood institute recipient epidemiology and donor evaluation study (REDS-III): a research program striving to improve blood donor and transfusion recipient outcomes. *Transfusion* 54: 942–955.
24. Grifoni, A., J. Pham, J. Sidney, P. H. O'Rourke, S. Paul, B. Peters, S. R. Martini, A. D. de Silva, M. J. Ricciardi, D. M. Magnani, et al. 2017. Prior dengue virus exposure shapes T cell immunity to Zika virus in humans. *J. Virol.* 91: e01469-17.
25. Jensen, K. K., M. Andreatta, P. Marcatili, S. Buus, J. A. Greenbaum, Z. Yan, A. Sette, B. Peters, and M. Nielsen. 2018. Improved methods for predicting peptide binding affinity to MHC class II molecules. *Immunology* 154: 394–406.
26. Rombi, F., R. Bayliss, A. Tuplin, and S. Yeoh. 2020. The journey of Zika to the developing brain. *Mol. Biol. Rep.* 47: 3097–3115.
27. Elong Ngono, A., M. P. Young, M. Bunz, Z. Xu, S. Hattakam, E. Vizcarra, J. A. Regla-Nava, W. W. Tang, M. Yamabhai, J. Wen, and S. Shresta. 2019. CD4+ T cells promote humoral immunity and viral control during Zika virus infection. [Published erratum appears in 2019 *PLoS Pathog.* 15: e1007821.] *PLoS Pathog.* 15: e1007474.
28. Tonnerre, P., J. G. Melgaço, A. Torres-Cornejo, M. A. Pinto, C. Yue, J. Blümel, P. S. F. de Sousa, V. D. M. de Mello, J. Moran, A. M. B. de Filippis, et al. 2020. Evolution of the innate and adaptive immune response in women with acute Zika virus infection. *Nat. Microbiol.* 5: 76–83.
29. Muthivhi, T. N., M. G. Olmsted, H. Park, M. Sha, V. Raju, T. Mokoena, E. M. Bloch, E. L. Murphy, and R. Reddy. 2015. Motivators and deterrents to blood donation among Black South Africans: a qualitative analysis of focus group data. *Transfus. Med.* 25: 249–258.
30. Tscharke, D. C., G. Karupiah, J. Zhou, T. Palmore, K. R. Irvine, S. M. M. Haeryfar, S. Williams, J. Sidney, A. Sette, J. R. Bennink, and J. W. Yewdell. 2005. Identification of poxvirus CD8+ T cell determinants to enable rational design and characterization of smallpox vaccines. *J. Exp. Med.* 201: 95–104.
31. Sylwester, A. W., B. L. Mitchell, J. B. Edgar, C. Taormina, C. Pelte, F. Ruchti, P. R. Sleath, K. H. Grabstein, N. A. Hosken, F. Kern, et al. 2005. Broadly targeted human cytomegalovirus-specific CD4+ and CD8+ T cells dominate the memory compartments of exposed subjects. *J. Exp. Med.* 202: 673–685.
32. Grifoni, A., D. Weiskopf, S. I. Ramirez, J. Mateus, J. M. Dan, C. R. Moderbacher, S. A. Rawlings, A. Sutherland, L. Premkumar, R. S. Jadi, et al. 2020. Targets of T cell responses to SARS-CoV-2 coronavirus in humans with COVID-19 disease and unexposed individuals. *Cell* 181: 1489–1501.e15.
33. Lee, J., H. Tam, L. Adler, A. Ilstad-Minnihan, C. Macaubas, and E. D. Mellins. 2017. The MHC class II antigen presentation pathway in

human monocytes differs by subset and is regulated by cytokines. *PLoS One* 12: e0183594.

34. Hanajiri, R., G. M. Sani, P. J. Hanley, C. G. Silveira, E. G. Kallas, M. D. Keller, and C. M. Bollard. 2019. Generation of Zika virus-specific T cells from seropositive and virus-naïve donors for potential use as an autologous or "off-the-shelf" immunotherapeutic. *Cytotherapy* 21: 840–855.
35. Jones, D., C. N. Como, L. Jing, A. Blackmon, C. P. Neff, O. Krueger, A. N. Bubak, B. E. Palmer, D. M. Koelle, and M. A. Nagel. 2019. Varicella zoster virus productively infects human peripheral blood mononuclear cells to modulate expression of immunoinhibitory proteins and blocking PD-L1 enhances virus-specific CD8+ T cell effector function. *PLoS Pathog.* 15: e1007650.
36. James, E. A., J. A. DeVoti, D. W. Rosenthal, L. J. Hatam, B. M. Steinberg, A. L. Abramson, W. W. Kwok, and V. R. Bonagura. 2011. Papillomavirus-specific CD4+ T cells exhibit reduced STAT-5 signaling and altered cytokine profiles in patients with recurrent respiratory papillomatosis. *J. Immunol.* 186:6633–6640.
37. Strickland, N., T. L. Müller, N. Berkowitz, R. Goliath, M. N. Carrington, R. J. Wilkinson, W. A. Burgers, and C. Riou. 2017. Characterization of Mycobacterium tuberculosis–specific cells using MHC class II tetramers reveals phenotypic differences related to HIV infection and tuberculosis disease. *J. Immunol.* 199: 2440–2450.
38. Moss, N. J., A. Magaret, K. J. Laing, A. S. Kask, M. Wang, K. E. Mark, J. T. Schiffer, A. Wald, and D. M. Koelle. 2012. Peripheral blood CD4 T-cell and plasmacytoid dendritic cell (pDC) reactivity to herpes simplex virus 2 and pDC number do not correlate with the clinical or virologic severity of recurrent genital herpes. *J. Virol.* 86: 9952–9963.
39. Weiskopf, D., K. S. Schmitz, M. P. Raadsen, A. Grifoni, N. M. A. Okba, H. Endeman, J. P. C. van den Akker, R. Molenkamp, M. P. G. Koopmans, E. C. M. van Gorp, et al. 2020. Phenotype and kinetics of SARS-CoV-2-specific T cells in COVID-19 patients with acute respiratory distress syndrome. *Sci. Immunol.* 5: eabd2071.
40. Zaunders, J. J., M. L. Munier, N. Seddiki, S. Pett, S. Ip, M. Bailey, Y. Xu, K. Brown, W. B. Dyer, M. Kim, et al. 2009. High levels of human antigen-specific CD4+ T cells in peripheral blood revealed by stimulated coexpression of CD25 and CD134 (OX40). *J. Immunol.* 183: 2827–2836.
41. Trück, J., R. Mitchell, A. J. Thompson, B. Morales-Aza, E. A. Clutterbuck, D. F. Kelly, A. Finn, and A. J. Pollard. 2014. Effect of cryopreservation of peripheral blood mononuclear cells (PBMCs) on the variability of an antigen-specific memory B cell ELISpot. *Hum. Vaccin. Immunother.* 10: 2490–2496.
42. Martikainen, M.-V., and M. Roponen. 2020. Cryopreservation affected the levels of immune responses of PBMCs and antigen-presenting cells. *Toxicol. In Vitro* 67: 104918.
43. Blom, K., M. Braun, M. A. Ivarsson, V. D. Gonzalez, K. Falconer, M. Moll, H. G. Ljunggren, J. Michaëlsson, and J. K. Sandberg. 2013. Temporal dynamics of the primary human T cell response to yellow fever virus 17D as it matures from an effector- to a memory-type response. *J. Immunol.* 190: 2150–2158.
44. Graham, N., P. Eisenhauer, S. A. Diehl, K. K. Pierce, S. S. Whitehead, A. P. Durbin, B. D. Kirkpatrick, A. Sette, D. Weiskopf, J. E. Boyson, and J. W. Botten. 2020. Rapid induction and maintenance of virus-specific $CD8^+$ T_{EMRA} and $CD4^+$ T_{EM} cells following protective vaccination against dengue virus challenge in humans. *Front. Immunol.* 11: 479.
45. Geiger, R., T. Duhen, A. Lanzavecchia, and F. Sallusto. 2009. Human naive and memory CD4+ T cell repertoires specific for naturally processed antigens analyzed using libraries of amplified T cells. *J. Exp. Med.* 206: 1525–1534.
46. Wölfl, M., J. Kuball, M. Eyrich, P. G. Schlegel, and P. D. Greenberg. 2008. Use of CD137 to study the full repertoire of CD8+ T cells without the need to know epitope specificities. *Cytometry A* 73: 1043–1049.
47. Koblischke, M., K. Stiasny, S. W. Aberle, S. Malafa, G. Tsouchnikas, J. Schwaiger, M. Kundi, F. X. Heinz, and J. H. Aberle. 2018. Structural influence on the dominance of virus-specific CD4 T cell epitopes in Zika virus infection. [Published erratum appears in 2018 *Front. Immunol.* 9: 2083.] *Front. Immunol.* 9: 1196.
48. Dhanda, S. K., K. Vaughan, V. Schulten, A. Grifoni, D. Weiskopf, J. Sidney, B. Peters, and A. Sette. 2018. Development of a novel clustering tool for linear peptide sequences. *Immunology* 155: 331–345.